

Comparison of single-shot 2D EPI and segmented 3D EVI acquisition for fMRI at 7T

W. van der Zwaag^{1,2}, T. Kober^{1,3}, J. P. Marques^{1,2}, G. Glover⁴, R. Gruetter^{1,5}, and G. Krueger³

¹LIFMET, EPFL, Lausanne, Switzerland, ²UNIL, Lausanne, Switzerland, ³Advanced Clinical Imaging Technology, Siemens Suisse SA - CIBM, Lausanne, Switzerland,

⁴Stanford University, Stanford, United States, ⁵UNIL/UNIG, Lausanne/Geneva, Switzerland

Introduction

Echo volumetric imaging (EVI) has been demonstrated to be an attractive tool for high spatio-temporal fMRI^{1,2,3}. Compared to 2D single shot acquisitions, EVI benefits from increased SNR due to the volume excitation³. At the same time, however, increased signal fluctuations (physiological noise) have been observed in segmented 3D spiral fMRI investigations⁴, which counteract the SNR gain of the 3D acquisitions. In this work, we compare the performance of a single-shot 2D EPI and a segmented 3D EVI acquisition for fMRI at 7T. In particular, we (i) investigated the physiological noise properties of both techniques in phantom and humans and (ii) compared activation maps from fMRI experiments using a visual checkerboard task.

Methods

Four subjects and an oil phantom were scanned at 7T (Magnetom Tim 7T, Siemens, Germany) using a head gradient insert and an 8 channel RF-coil (Rapid, Germany). For all experiments, 50 temporal volumes were acquired. Segmented EVI volumes consisted of 30 slices (30 segments), multi-slice volumes consisted of 15 interleaved slices with 2 mm gap, to eliminate the effect of an imperfect slice profile. In both cases, acquisition of a full volume required 3s ($TR_{segment3D}/\alpha_{3D}=100ms/18^\circ$, $TR_{2D}/\alpha_{2D}=3s/90^\circ (\geq 64^\circ \text{ in fMRI})$). In the fMRI experiments, α_{2D} was adapted when SAR limitation was exceeded (min 64 $^\circ$). For 3D scans a 5-lobe sinc pulse was used to achieve a good slab profile. Other parameters were the same: TE = 28, GRAPPA = 2 and for the fMRI experiments: 2*2*2 mm resolution, matrix size 96 * 96 and bandwidth 1698 Hz/px. The paradigm involved a visual task with: 10s ON, 20s OFF, repeated 5 times. fMRI processing of the 3D data considered only odd slices to keep matrix sizes and slice distribution equal to the 2D experiments.

For the physiological noise analysis, data were acquired with voxel sizes of 1.5*1.5*2, 2*2*2, 3*3*2 and 5*5*2, matrix size 96*96 and bandwidth 1408 Hz/px apart from the 1.5*1.5*2 data, which had a matrix size 128*128 and BW 1698. In 2 cases the SAR limit was reached for the 2D scans. In those cases, the number of slices was reduced (min 8). SNR was measured as the mean signal in a parietal white matter ROI over the standard deviation of an ROI placed outside the brain/phantom and outside the area of expected Nyquist ghost. tSNR was measured as the mean ratio of signal over temporal variation in the WM ROI. λ , a measure of sensitivity to signal fluctuations⁵, was obtained from a non-linear least squares fit to: $tSNR = SNR / \sqrt{1 + \lambda^2 SNR^2}$. Finally, Nyquist ghosting was measured as: Ghost = $(S_{ROIghost} - S_{ROInoise}) / S_{ROIWM}$ with ROI_{ghost} a ~100 voxel ROI in the maximum Nyquist ghost area.

Results

Activation was consistently found in the visual cortex. On average, the maximum z-score in activation maps from the 3D acquisition was higher than from 2D acquisitions (11.2 vs. 9.3) (Figure 1). In addition, an 87% increase in size of the active region was found in the 3D scans. Susceptibility induced distortions were similar for the two acquisitions schemes as can be judged from the images shown in Figure 1. Nyquist ghosting was also comparable, 3.4% and 2.4% on average for the 2D and 3D data shown in Figure 1. With respect to signal fluctuations, SNR values were 70% higher in segmented 3D data compared to 2D data in humans. Interestingly, asymptotic limits of tSNR values were significantly lower for 3D than for 2D (Figure 2), indicating a stronger sensitivity to physiological noise fluctuations in the segmented 3D scan. In phantom data, 2D and 3D data fell on the same SNR/tSNR curve with $\lambda = 0.0030 (\pm 0.0007)$. In humans, λ_{2D} was 0.0085 (± 0.0010) and λ_{3D} 0.019 (± 0.005) (95% confidence bounds).

Discussion

Improvements in SNR and BOLD contrast were comparable to those found in experiments with a 2D or 3D spiral readout⁴. Our investigations of the tSNR, however, demonstrated that signal fluctuations/physiological noise contributions are clearly increased in segmented acquisition schemes. Since this is not obvious in phantom scans, we speculate these additional fluctuations stem from true physiological origin, i.e. respiration and cardiac pulsations effects, which agrees with our observation that difference in temporal signal variance between gray and white matter is larger for the 3D acquisitions (data not shown). Respective signal fluctuations contribute differently to segmented 3D and 2D multi-slice acquisitions. In 3D, all slices experience identical respiration contributions, whereas for multi-slice data, each slice is affected separately. Some of the respiration effects can be compensated for by monitoring the respiration curve or by navigator corrections, techniques that have not been applied in the presented data. Noteworthy, segmented EVI is less sensitive to spin history artifacts than multi-slice EPI, but large bulk motion may result in other artifacts.

The increase in BOLD sensitivity is significant, but, as physiological noise becomes dominant quickly at signal strengths typically seen at high B_0 ($>3T$), fMRI protocols using segmented EVI at high B_0 should take this into account by limiting the protocol parameters to stay in a thermal-noise dominated regime. This may be achieved, e.g. using small voxels⁶.

Conclusion

Segmented EVI offers higher SNR, higher BOLD sensitivity but is more susceptible to physiological noise degradation. Moreover, EVI achieves significantly lower SAR levels compared to multi-slice single-shot EPI at 7 T because of the smaller flip angle.

References

¹van der Zwaag, 2006, MRM, ²Witzel 2008 ISMRM proc, ³Rabrait 2008 ISMRM proc, ⁴Lai, 1998, MRM, ⁵Kruger, 2001, MRM, ⁶Hu, 2007, MRM.

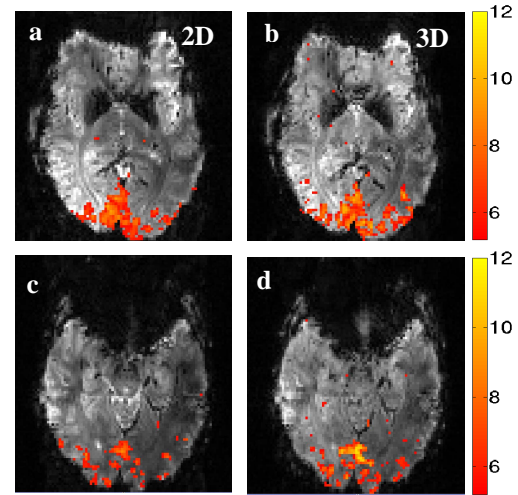


Figure 1 Z-score maps ($p_{cor} < 0.05$) from representative subjects shown overlaid on an image from the fMRI train. (a) subject 1, 2D (b) subject 1, 3D (c) subject 2, 2D (d) subject 2, 3D.

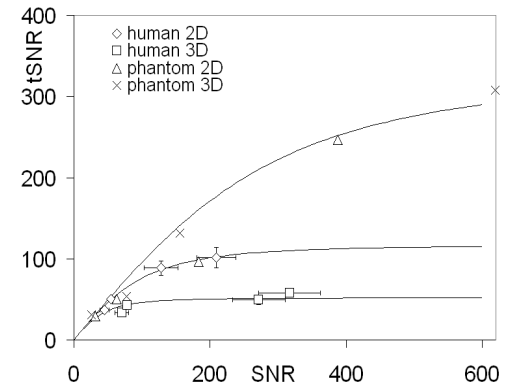


Figure 2 tSNR as a function of SNR in phantom data and WM ROIs. Error bars indicate the standard error over subjects.